Acute effects of quinoline and 2-methylquinoline on electrical activity of great pond snail (*Lymnaea stagnalis*) neurons

by

Cameron Tramley

A thesis submitted to the Department of Biological Sciences, University of Manitoba,

in partial fulfilment of the requirements for the course

BIOL 4100 (Honours Thesis)

for the degree of

Bachelor of Science (Honours)

Abstract

Polycyclic aromatic compounds (PAC) are organic compounds found ubiquitously in the environment and originate naturally or anthropogenically. They are persistent, bioaccumulative, and toxic (PBT). PACs have been found to modulate voltage gated ion channels in fish cardiomyocytes. Many studies have examined PACs effects, however, there is growing concern about a less studied class of PACs: hetero-polycyclic aromatic compounds (HPACs). Quinoline and its derivative 2-methylquinoline are two-ringed HPACs found in high concentrations in sediment and tissues of fishes from the Great Lakes. Studies investigating synthetic quinoline derivatives used in the pharmaceutical industry have shown HPACs modulate voltage gated sodium, calcium and potassium ion channels in cardiomyocytes of fishes and mollusk neurons. We therefore designed a study investigating the acute neurobiological effects of quinoline and 2-methylquinoline on Great Pond Snail (*Lymnaea stagnalis*) neurons, a model with a large easily accessible central nervous system and well conserved ion channels. Electrophysiological characteristics were measured by performing suction electrode experiments on the right internal nerve of the right parietal *Lymnaea stagnalis* ganglion. Extracellular recordings before and after application of various quinoline or 2-methylquinoline concentrations were used to determine the frequency of right parietal nerve activity which we normalized as percent of control. The extracellular recordings revealed that quinoline affects right parietal nerve activity in a dose dependent manner. Quinoline caused a statistically significant effect on right parietal nerve activity at 1000 nM, but not 100 nM, and 10 nM, with mean percent of control values being 89.2 ± 4.3%, 103.9 ± 4.6% and 99.9 ± 3.5% respectively. 2-Methylquinoline had no statistically significant effect on right parietal nerve activity at 1000 nM. These experiments highlight the importance of understanding the neurobiological effect of PBT environmental contaminants

quinoline and 2-methylquinoline, as well as demonstrate the utility of suction electrode recordings as an electrophysiology technique to evaluate acute neurotoxicity of environmental contaminants.

Acknowledgements

I would like to express my sincere gratitude to my supervisor, Dr. Mark Fry for all his assistance throughout my Honours. I would also like to thank the other members of my Thesis committee, Dr. Gregg Tomy and Dr. John Markham, for agreeing to be on the committee and their support throughout. Dr. Tomy's lab and Nipuni Vitharana also provided crucial help by providing the chemicals I used in performing my experiments as well as fundamental environmental data. Last, I would like to thank the Animal Care Facility at the University of Manitoba for taking care of and providing the snails used in this study.

Table of Contents

List of Figures

1. Introduction

1.1 Polycyclic aromatic compounds: sources and distribution

Polycyclic aromatic compounds (PACs), organic compounds containing at least two fused benzene rings, are found ubiquitously in the environment, with either natural or anthropogenic sources (Abdel-Shafy and Mansour 2016; Figure 1; Berthiaume et al. 2021). Pyrogenic PACs result from incomplete carbon material combustion that can either be anthropogenic (e.g., incomplete fuel combustion from motored vehicles or watercraft) or natural (e.g., forest fires) (Abdel-Shafy and Mansour 2016; Marvin et al. 2021). Petrogenic PACs are derived from petroleum (e.g., crude oil and coal) (Wang et al. 2014; Andersson and Achten 2015). Plants and bacteria can also synthesize PACs through the anabolism of carbon material (Abdel-Shafy and Mansour 2016). Studies of the Great Lakes, Canadian Arctic, and Alberta oil sands region show an ongoing trend of increasing PACs levels (Marvin et al. 2021; Vitharana et al. 2024). The hydrophobicity of PACs helps facilitate their release into the environment through atmospheric deposition or runoff by adhering to particulate matter (Kimbrough et al. 2021). Extensive research on PACs since the early 1970s has labelled them as environmentally persistent, bioaccumulative, and toxic (PBT), and has led to their addition to the Canadian Environmental Protection Act (CEPA) toxic substances list in 1994 (Marvin et al. 2021; Vitharana et al. 2024).

1.2 PACs: acute toxicity studies

Studies have examined the health effects of PACs. Adult Zebrafish (*Dani rerio*) exposed to PACs in their diet had a dose dependent decrease in metabolic rate and oxygen transport resulting in disrupted cardiac function (Lucas et al. 2016). F-344 rats given single doses (25-200 mg/kg^{-1}) of the PAC benzo(a)pyrene showed significant dose-related motor ability decreases from oxidative stress in the striatum and hippocampus through the inhibition of the antioxidant scavenging system and increase in lipid peroxidation (Saunders et al 2006). Oxidative stress was also observed in their central nervous system (CNS) through the formation of reactive oxygen species (ROS) formed during *o*-quinone redox reactions, a product of benzo(a)pyrene metabolism (Saunders et al 2006). Intra-striatal and intra-hippocampal micro-injections of fractioned diesel exhaust containing various PACs (concentration corresponding to diesel exhaust from a truck driving 19.5 meters) caused lesions characterised by astrogliosis and tissue loss in the striatum and hippocampus of Sprague-Dawley rats (Andersson et al. 1998). Potential health effects of acute exposure to PACs have been demonstrated, however, the mechanism of toxicity is not well understood.

1.3 PACs modulate action potentials acutely

Electrophysiological studies on PACs have demonstrated PACs may modulate ion channel activity (Kompella et al. 2021; Vehniäinen et al. 2019). In whole-cell patch clamp experiments, the PAC phenanthrene dose-dependently shortened action potential durations in zebrafish cardiomyocytes (Kompella et al. 2021). Phenanthrene exposure dose-dependently reduced calcium ion influx by blocking L-type calcium ion current, and to a lesser extent blocked the rapid delayed rectifier potassium current, a current important in action potential

repolarization and deactivation (Kompella et al. 2021). Together these effects resulted in shortened action potential durations (Kompella et al. 2021). Another whole-cell patch clamp experiment, using cardiomyocytes from rainbow trout (*Oncorhynchus mykiss*), found that exposure to PACs phenanthrene and retene caused a dose dependent increase in the inward sodium current but decreases in L-type calcium ion current and to a lesser extent decreased the rapid delayed rectifier potassium current (Vehniäinen et al. 2019). Together the net effect of these were reduced action potential durations, impairing the contractility of myocytes, thereby impairing their cardiac function (Vehniäinen et al. 2019). These findings are further supported by studies showing phenanthrene dose-dependently blocked the rapid delayed rectifier potassium current and reduced L-type calcium ion current, resulting in a decrease in cardiac force and rhythm disruption in cardiomyocytes from mackerel and yellowfin tuna (Brette et al. 2017). These findings suggest a mechanism of acute cardiotoxicity in cardiomyocytes from exposure to PACs (Kompella et al. 2021; Vehniäinen et al. 2019). The fact these compounds modified voltage gated ion currents suggests that central nervous system neurons expressing similar ion channels may also be affected given that alteration of neuronal electrical activity during development can have catastrophic effects on adult brains (Smith et al. 2018), and with environmental PAC concentrations increasing, investigating the effects of PACs on neurons is critically important today (Vitharana et al. 2024). Historically, studies have focused on the sixteen PACs in the CEPA toxic substances list, with significantly less focus on other compounds such as hetero-polycyclic aromatic compounds (HPACs) known to have PACs-like effects, or worse (Vitharana et al. 2024).

1.4 HPACs

HPACs differ from PACs structurally, as one of their carbons is replaced by a sulfur, oxygen, or nitrogen atom, making them more water soluble than other PACs and increasing their mobility and thus potential toxicity (Figure 1; Neuwoehner et al. 2009; Brinkmann et al. 2014). Like PACs, HPACs can come from anthropogenic or natural sources and are found at sites with PACs such as former gas work manufacturing and wood preservation sites (Neuwoehner et al. 2009; Peddinghaus et al. 2012; Brinkmann et al. 2014). There is limited knowledge on their environmental occurrence, distribution and toxicological significance and further investigation is therefore important (Andersson and Achten 2015; Peddinghaus 2012; Vitharana et al. 2024).

1.5 HPACs of concern: Quinoline and its derivative 2-methylquinoline

Two HPACs found in high concentrations in the Great Lakes are of concern and merit investigation: quinoline and its derivative 2-methylquinoline (Canada Health 2010; Canada, Environment and Climate Change 2011; Vitharana et al. 2024). Structurally, quinoline is a benzene ring fused to a pyridine ring containing a nitrogen atom (Figure 1; Vitharana et al. 2024). 2-methylquinoline structurally differs from quinoline in that a methyl group has been added at position two (Figure 1; Boersma 2009). Quinoline and 2-methylquinoline can be found in coal-tar and coal-tar related products and is used to treat wood and make paints or dyes (Canada Health 2010; Luongo et al. 2014). In addition, quinoline and its derivatives have been widely used in the pharmaceutical industry (Zhao et al., 2023). Quinine, a quinoline derivative found in the bark of the plant cinchona, has been widely used as an antimalarial drug (Zhao et al., 2023). Another quinoline derivative called chloroquine has been widely used as an anti-viral or anti-parasitic drug (Zhao et al., 2023). Quinoline and 2-methylquinoline can be made

synthetically through the Skraup reaction which is, in brief, the reaction when sulfuric acid reacts with aniline, nitrobenzene and glycol in the presence of an oxidizing agent (U.S. Environmental Protection Agency 1985). Quinoline shows a high transport potential in water of over 1500 kilometres but shows a moderate transport potential in air of only 332 kilometers (Environment and Climate Change 2011). Quinoline has been shown to be environmentally persistent, as sediment cores from Lake Washington and Puget Sound in the United States dating back over a century contained quinoline (Furlong and Carpenter 1982). With quinoline's increased water solubility compared to PACs such as naphthalene, and its tendency to associate with particulate organic matter because of the nitrogen atom within its aromatic ring, quinoline has higher mobility in water and soil (Environment and Climate Change 2011; Fowler et al. 1994). Quinoline is easily biodegradable in aerobic soil where it is broken down by microorganisms, but with its high solubility and mobility in soil, quinoline can move deeper to more anaerobic soils easily, leading to low biodegradation and environmental persistence (Fowler et al. 1994; Environment and Climate Change 2011). Some studies have shown quinoline having a low bioaccumulation potential, evidenced by the bioconcentration of quinoline in the fathead minnow (*Pimephales promelas*) of only a factor of eight which, according to CEPA, does not meet the requirements for classification as a chemical that bioaccumulates (>5000 L·kg−1 bioconcentration factor) (Southworth et al. 1980; Environment and Climate Change 2011). Some ongoing studies question the validity and accuracy of these data (Arnot and Gobas 2006; Vitharana et al., 2025, unpublished raw data).

Human activity is the main cause of quinoline release into the environment, including incomplete coal and petroleum combustion and industrial site coal tar and creosote leakage (Canada Health 2010; Brinkmann et al. 2014). There is growing evidence that quinoline is found

throughout the environment (Chen and Preston 1998). It has been detected in water samples from a contaminated site in Saint Louis Park, Minnesota (Minnesota Pollution Control Agency 2011). A recent study analyzing Randle Reef, Hamilton, Ontario sediment samples found many HPACs including quinoline and 2-methylquinoline (Vitharana et al. 2024). Quinoline has also been found in the atmosphere, where samples of outdoor air in Columbus, Ohio contained measurable levels of quinoline (26 $\mu g \cdot m^{-3}$) (Chuang et al. 1991). Human exposure to quinoline occurs mainly through the inhalation of smoke from either tobacco or incomplete combustion of both coal and coal-related products (Canada Health 2010; U.S. Environmental Protection Agency 2001).

1.6 Metabolism of Quinoline

Humans metabolize quinoline, evidenced by *in vitro* experiments of human microsomes expressing cytochrome P450 enzyme CYP2EI, responsible for mediating the metabolization of quinoline to 3-hydroxyquinoline (Reigh et al. 1996; U.S. Environmental Protection Agency 2001). When quinoline is administered to dogs intravenously, only 0.5% of unchanged quinoline is found in the urine, suggesting it is almost completely metabolized, with one metabolite being 3-hydroxyquinoline (Novak and Brodie 1950). Administration of quinoline to dogs resulted in detectable levels of 2-methylquinoline in urine (Tamura 1923, as cited in Novak and Brodie 1950). There is no literature directly demonstrating the metabolism of 2-methylquinoline by human hepatic cells, but, with the similarities between dog and human livers and given it is found in the environment along with quinoline and 2-methylquinoline, it seems a likely derivative (Vitharana et al. 2024; Tamura 1923 as cited in Novak and Brodie 1950). Given the environmental accumulation and known toxic effects of related HPACs, further investigation into the physiological effects of quinoline and its derivative 2-methylquinoline is warranted.

1.7 Quinoline and 2-methylquinoline toxicity studies

Studies have investigated the health effects of quinoline and its derivatives. In an *in vivo* experiment, lacZ mice were injected intraperitoneally with a 50 mg/kg dose of quinoline each day for four days (Suzuki et al. 1998). Using lacZ as a reporter gene for mutagenesis, quinoline treatment increased the frequency of mutations in hepatic cells and promoted tumour growth, demonstrating the carcinogenic and mutagenic nature of quinoline (Suzuki et al. 1998). Male Wistar rats given quinoline at high concentrations of 0.25% of their body weight in their diets for twelve weeks developed hemangioendotheliomas in their livers, also demonstrating the carcinogenic behaviour of quinoline (Hasegawa et al. 1989). When quinoline and 2-methylquinoline (7.5 mg) were applied to the skin of SENCAR mice, tumours developed after 23 weeks in 53% of the mice given quinoline and in 6.7% of the mice given 2-methylquinoline (Lavoie et al. 1984). *Salmonella typhimuriam* strain TA100 exposed to quinoline resulted in mutagenesis through frameshift mutations in a dose dependent manner (Neuwoehner et al. 2009; Suzuki et al. 1998). Chinese hamster lung cell linings treated with quinoline showed high levels of chromosomal aberrations, demonstrating quinoline's clastogenic nature (Suzuki et al. 2007).

1.8 Quinoline and its derivatives: acute effects on excitable cells

Studies on quinoline derivatives quinine, quinidine and chloroquine demonstrated HPACs may acutely modulate ion channels and disrupt action potentials in excitable cells (Ducouret 1976; Nawrath and Eckel 1979; Wang and Parker 1980). In microelectrode intracellular experiments, quinoline derivative quinidine sulfate, a drug previously used to treat cardiac arrhythmias, dose-dependently prolonged action potential durations in human

cardiomyocytes (Nawrath and Eckel 1979). Quinidine sulfate dose-dependently reduced inward sodium ion conductance through the modulation of voltage-gated sodium ion channels, leading to reductions in upstroke velocity of action potentials in human cardiomyocytes (Nawrath and Eckel 1979). Quinidine dose-dependently reduced potassium ion conductance through voltage-gated potassium channels modulation, leading to prolonged terminal repolarization phases in action potentials of human cardiomyocytes (Nawrath and Eckel 1979). Together, these findings demonstrate quinidine dose-dependently disrupted the cardiac function of human cardiomyocytes.

A study using whole-cell patch clamp experiments using microelectrode intracellular recording of cardiomyocytes from the edible frog (*Rana esculenta*) found quinidine sulfate exposure decreased the inward sodium ion conductance and slow inward calcium ion conductance (Ducouret 1976). In addition, quinidine sulfate exposure decreased reactivation kinetics of the sodium inward current, but increased the time required for activation and inactivation of inward sodium currents in frog cardiomyocytes which, together, reduced total action potential amplitude, prolonged the action potential tail and increased the effective refractory period, and quinidine exposure therefore disrupted the electrical excitability of frog cardiomyocytes (Ducouret 1976). These findings are further supported by microelectrode experiments on isolated canine Purkinje fibers, found quinidine dose-dependently decreased upstroke velocity of action potentials, increased the duration of the effective refractory period, and suppressed the spontaneous activity of the Purkinje fibres (Wang and Parker 1980).

These findings indicate a mechanism of cardiotoxicity in human, frog, and dog cardiomyocytes as the result of exposure to the quinoline derivative quinidine (Ducouret 1976; Nawrath and Eckel 1979; Wang and Parker 1980). As with PACs, these compounds modify

voltage gated ion currents, suggesting that neurons of the central nervous system expressing similar ion channels may also be affected.

Two studies performing whole-cell patch clamp experiments investigating the effects of quinoline derivatives on the excitability of molluscan neurons through modulation of voltage gated ion channels (Walden and Speckmann 1981; Hermann and Gorman 1984). Quinine caused a dose dependent decrease in the calcium ion dependent potassium outward current and peak amplitude of the inward sodium ion current in Burgandy snail (*Helix pomatia*) neurons (Walden and Speckmann 1981). Furthermore, California sea hare (*Aplysia californica*) neurons exposed to quinidine caused a decrease in the inward sodium and calcium ion currents as well as a decrease in the outward potassium currents (Hermann and Gorman 1984). Together, these papers found that quinoline derivatives dose-dependently affected action potentials in mollusk neurons through the modulation of voltage gated ion channels.

Historically, studies on the effects of quinoline have focused on synthetic derivatives, however, few studies have investigated the acute neurobiological effects of anthropogenic HPACs found in the environment.

1.9 Research gaps, objective, and hypotheses

Several studies have investigated the toxicities of PACs, showing adverse effects such as disrupted cardiac function through decreased metabolic rate and oxygen transport in adult Zebra fish or oxidative stress in the hippocampus and striatum of rats exposed to PACs (Lucas et al. 2016; Saunders et al. 2006). Studies on the effects of PACs and synthetic HPACs on electrical activity of cardiac muscle also demonstrate a potential mechanism of neurotoxicity (Ducouret 1976; Nawrath and Eckel 1979; Wang and Parker 1980; Brette et al. 2017; Vehniäinen et al.

2019; Kompella et al. 2021). These studies on cardiomyocytes are directly applicable to neurons, as both cell types express overlapping types of voltage gated ion channels including voltage gated sodium and calcium ion channels. In addition, studies on the effects of synthetic HPACs on the electrical activity of mollusk neurons also demonstrate a potential mechanism of toxicity (Walden and Speckmann 1981; Hermann and Gorman 1984). However, there are gaps. Few studies have considered the neurotoxicity of anthropogenic HPACs found in the environment, especially their acute neurobiological effects. Increasing environmental concentrations of these anthropogenic HPACs merits further investigation into their acute neurobiological effects and whether they modulate neuronal activity. These data could help assess their risk to human health and the determine importance of monitoring them (Vehniäinen et al. 2019).

The objective of this research project is to use an accessible electrophysiology technique to evaluate quinoline's and 2-methylquinoline's acute effects on the neuronal activity of an invertebrate's neurons. If related PACs are known to modulate ion channel activity, we hypothesize that quinoline or 2-methylquinoline will dose-dependently affect the measurable neuronal activity of Great Pond Snail (*Lymnaea stagnalis* [*L. stagnalis*]) neurons. To test this hypothesis, we designed a detailed study involving suction electrode experiments where we investigated the acute effects of quinoline and 2-methylquinoline on the neuronal activity of the internal right nerve of the right parietal ganglion of the central nervous system (CNS) of *L. stagnalis*, hereafter referred to as right parietal nerve activity. *L. stagnalis* was chosen as a model because of its widespread use in ecotoxicological studies due to its sensitivity to environmental toxins such as toxic metals and PACs, large and easily accessible CNS and nerves, well conserved ion channels, and its widespread use in electrophysiology studies (Amorim et al. 2019; Sverdrup et al. 2006; Beekharry et al. 2015). In addition, *L. stagnalis* can be maintained

under laboratory conditions, have a long lifespan, high fecundity, and less strict animal controls compared to vertebrate animal models such as rats or mice. *L. stagnalis* is thus an appropriate organism for examining quinoline's and 2-methylquinoline's neurobiological effects.

2. Methods and Materials

2.1 Animals

Great pond snails (*Lymnaea stagnalis*), obtained from the Department of Biomedical and Molecular Sciences at Queen's University, Kingston, Ontario, Canada, were maintained in an aquaculture facility at the University of Manitoba. They were fed romaine lettuce and trout pellets and provided with oyster shells as substrate.

2.2 Dissection

An external recording solution (ERS) containing (in mM) 4.1 $CaCl_2$, 1.5 $MgCl_2$, 5.0 4-(Hydroxyethyl) piperazine-1-ethanesulfonic acid (HEPES), 1.7 KCl, 51.3 NaCl, and 5 D-glucose at a pH of 7.9 was used to carry out the *L. stagnalis* dissection and suction electrode extracellular electrophysiology experiments. Snails were anesthetized by injecting them with 0.4 mL of 0.5 M $MgCl_2$, a commonly used anesthetic causing muscle relaxation through magnesium ions competitively block calcium channels, reducing muscle fiber excitability (Do 2013). Full anesthesia was deemed when they no longer responded to touch. The dissection was carried out using the method described by Wyttenbach et al. (2022).

The CNS is comprised of a ring of nine ganglia and two buccal ganglia which connect posteriorly to the buccal mass, both of which are located posterior to the buccal mass (Figure 2). The dissection of the ganglia is achieved by pulling the mantle back and making a longitudinal incision from the midsection to the most anterior end of the body using micro scissors. The stomach, male reproductive system, and connecting nerves are cut and removed to allow easier access to the ganglia. The CNS is dissected out by cutting the esophagus and all connecting nerves. The CNS is then placed in ERS solution until the proteolytic enzyme treatment.

A proteolytic enzyme treatment is used to degrade and soften the connective tissue sheath that covers the CNS of *L. stagnalis*, making it easier to remove with forceps and help expose the ganglia to the environment. The proteolytic enzyme treatment begins by submerging the ganglia in the digestion enzyme from Streptomyces griseus Type XIV (Sigma-Aldrich, Oakville, Ontario) at a concentration of 0.4 mg/mL for 16 minutes at 30.5°C. The CNS was washed in ERS and then submerged in papain protease solution (Worthington Biochemical Inc, Lakewood, New Jersey) at a concentration of 1 mg/mL for 50 minutes at 30.5°C. After being washed in ERS, the connective sheath covering the ganglia was removed carefully using fine forceps and a scalpel. This facilitated access to treatment of the ganglia in the suction electrode experiments. The ganglia are then placed in a sylgard lined 35 x 10 mm polystyrene tissue culture dish (Falcon, Corning Incorporated, New York) filled with 2.0 mL of ERS. The cerebral commissure is cut and pinned on both sides using 0.2mm Minutien pins. The CNS being dorsal side up provides easy access to the right parietal ganglion and its connecting nerve for testing (Figure 2). The buccal ganglia are pinned to prevent the possibility of being sucked up by the recording electrode (Figure 2). To expose neuron cell bodies to the solution in the dish, the right parietal ganglion (RPG) is cut by making a longitudinal incision using a surgical scalpel. This ensures the treatment reaches the neurons and is not block by any sheath covering the ganglion. A 3D-printed insert is then placed into the dish and used as a holder for the pump tubing for efficient flow of solution over the CNS during the suction electrode electrophysiology experiments.

2.3 Electrophysiology and Experimental Protocol

All experiments were carried out on a vibration isolation breadboard table raised by four inflatable air bags. The CNS of *L. stagnalis* was pinned to a sylgard dish by minutien pins and

observed using a Nikon SMZ-U Stereoscopic with a zoom ratio of 1:10 and magnification of 5-10x. The CNS was positioned in the cell culture dish in a way that the nerve from the RPG is accessible by suction electrode. The suction electrodes were made from fire polished thin-walled borosilicate glass with an outside diameter of 1.5 mm, inside diameter of 1.10 mm, length of 10 cm, and containing an inner filament (Sutter Instruments, Novato, California, USA). The electrodes were pulled using a P-97 Flaming/Brown Micropipette Puller (Sutter Instruments, Novato, California, USA). Using a ceramic square, the tip of the electrode was cut off carefully and heat polished, resulting in the desired diameter of approximately 200-250 μm. The recording apparatus was comprised of a suction electrode fitted into a Model 3000 headstage (A-M systems, Hinckley, United Kingdom) containing a chlorinated silver wire. The headstage was held in place and controlled by a micromanipulator (Narishige, Japan). The suction electrode apparatus was comprised of the electrode, the headstage, the micromanipulator, and polyethylene tubing that connects the headstage to a 3 mL syringe. The micromanipulator was used to place the suction electrode in line with the nerve where negative pressure was applied using the syringe connected to the headstage by plastic tubing, resulting in approximately one-third of the nerve being sucked up into the electrode. Once a good seal between the nerve and the electrode was established, right parietal nerve activity was amplified and sampled using a Model 3000 AC/DC Differential Amplifier (A-M systems) with a high pass filter at 1.0 Hz, a low pass filter at 1 kHz, a 60 Hz notch filter and a signal gain of 500. Next, the data was digitized with a Digidata 1322A (Axon Instruments Inc) at a rate of 500 kHz and recorded by a computer running the WinEDR V.4.0.1 software (Strathclyde, Glasgow, Scotland).

A peristaltic pump system was used to facilitate flow of ERS, or ERS containing tricaine methanesulfonate (MS222; Syndel), vehicle dimethyl sulfoxide (DMSO; Sigma), or

experimental concentrations of quinoline or 2-methylquinoline (Centre for Oil and Gas Research and Development) dissolved in DMSO over the CNS while right parietal nerve activity was recorded. A linear flow of solution over the CNS at a flow rate of 1.3 mL/min was established by placing the inflow tube and outflow tube 180 degrees from each other, with identical flow rates.

Our preliminary experiments used MS222, a known voltage-gated sodium channel blocker, in ERS as a positive control to first demonstrate the electrical signals recorded were of *Lymnaea* neurons. Second, it would show the timing of how a single molecule can affect the right parietal nerve activity of *L. stagnalis.* Lastly, in the presence of a complete nerve block, it would reveal the signal to noise ratio and true baseline showing electrical noise without any physiological signals. In addition, the experiments helped optimize our setup.

Preliminary experiments already performed in our lab consisting of washing 38.3 mM MS222 over the CNS of *L. stagnalis* for ten minutes have demonstrated that we are recording right parietal nerve activity (Figure 3). We have been able to observe the known effects of MS222 on electrical activity in organisms with the increase in right parietal nerve activity after application, followed by the sharp attenuation of activity (Figure 3).

We then tested effects of doses of quinoline and 2-methylquinoline on the right parietal nerve activity in *L. stagnalis*. As outlined in Figure 4, the experimental protocol began with the nerve being captured by the suction electrode. The CNS was then allowed to settle for three minutes with the application of ERS only to establish a stable recording (control). This was followed by a ten-minute control using ERS containing 0.1% DMSO vehicle, which acted as a control to demonstrate the stability of our recordings. Next, 10 mL of HPAC (quinoline or 2-methylquinoline) was washed over the CNS. Three concentrations (1000 nM, 100 nM, 10 nM) of quinoline and one concentration (1000 nM) of 2-methylquinoline were used. The HPAC

solutions were prepared using a serial dilution. The rationale for a serial dilution is to maintain a constant volume of DMSO (0.1%) in all dilutions. One mM Stock quinoline and 2-methylquinoline were prepared in 0.1% DMSO. The HPAC treatment was then followed by washing over the experimental unit with ERS containing 0.1% DMSO for a minimum of three minutes to ensure the HPAC had been washed out thoroughly. Finally, 38.3 mM of MS222 containing 0.1% DMSO was washed over the CNS to establish a noise-free baseline for the experiment. We performed seven MS222 control experiments (n=7), and ten experiments (n=10) for each treatment of HPAC, replicating numbers common in the literature for extracellular recordings on *L. stagnalis* nerves (Nezlin and Voronezhskaya 1997).

2.4 Data Analysis and Statistical Analysis

A series of extracellular recordings of right parietal nerve activity were evaluated and analyzed by the Spike2 software (Cambridge Electronic Design Limited). The signal to noise ratio of the recordings was improved using digital filter in Spike2 software. The frequency of right parietal nerve activity was calculated before and after MS222 treatment (positive control). In brief, pairs of vertical cursors were placed 100 seconds apart at two sections of the MS222 experiment, one during the ERS negative control, and the second when the right parietal nerve activity had stopped. Frequency represents the number of events (action potentials from a single or many neurons firing) crossing a threshold during the 100 seconds, where any events that cross the line within 0.01 second are considered one event of right parietal nerve activity (Figure 5). The threshold was placed at least five standard deviations above the mean of the physiological activity free baseline after MS222 treatment. This method of placing the threshold at least five standard deviations above the mean will miss some real biological events, but we are confident it is the best method for not including what we have concluded is non physiological noise, reducing

the likelihood that any potential effect is lost in the electrical noise. The frequency of right parietal nerve activity before and after quinoline and 2-methylquinoline treatments was determined using techniques similar to the MS222 experiments, but the pairs of vertical cursors were spaced 250 seconds apart, with one pair being placed during ERS containing 0.1% DMSO control and the other toward the end of the HPAC treatment.

The frequencies of right parietal nerve activity before and after MS222 treatment, quinoline (1000 nM, 100 nM and 10 nM), and 2-methylquinoline (1000 nM) were presented as three separate line graphs (Figure 8A; Figure 10B; Figure 12B). We also expressed the data as percent in activity after treatment compared to control. The percent change of control for MS222, quinoline (1000 nM, 100 nM and 10 nM), and 2-methylquinoline (1000 nM) were determined and normalized, and box plot graphs were generated (Figure 8B; Figure 11; Figure 13).

Preplanned paired sample t-tests ($p<0.05$) were performed on frequencies of right parietal nerve activity before and after MS222, quinoline for each dose, and 2-methylquinoline, to determine if there was a significant difference between frequency means of control and treatment. One sample t-tests ($p<0.05$) were performed on percent of control for MS222, quinoline for each dose, and 2-methylquinoline to determine if there was a significant difference between means of control and treatment. The means are presented as ± the standard error of the mean (SEM).

3. Results

3.1 Extracellular recordings of MS222 treatment reveal right parietal nerve activity

We performed a positive control experiment using MS222. The experiment had three parts: the first part was washing ERS over the CNS for 10-minutes to establish a stable baseline, the second involved switching to ERS (negative control) for 5-minutes, and the third once the right parietal nerve activity was stable the CNS was exposed to 38.3 mM MS222 (Figure 7A). We examined and plotted the effects 38.3 mM MS222 (n=7) on right parietal nerve activity. MS222 exposure resulted in a characteristic increase in right parietal nerve activity followed by a sharp attenuation of neuronal activity (Figure 7A). Figure 7B demonstrates a typical extracellular recording of right parietal nerve activity in *L. stagnalis*. Blocking right parietal nerve electrical activity after MS222 treatment can be observed in Figure 7C, where the flat baseline indicates the cessation of all right parietal nerve activity. The biological "*activity free*" baseline after MS222 treatment was used to determine the threshold of electrical events of right parietal nerve activity for each of the experiments. The mean frequency of right parietal nerve activity after MS222 treatment compared to control was $0.013 \pm 0.010\ s^{-1}$, which was significantly less than control at $9.6 \pm 1.7\ s^{-1}$ ($p=0.00134$, $n=7$, paired t-test).

The data were normalized and expressed as percent in right parietal nerve activity after 38.3 mM MS222 compared to control (ERS), where 100% represents the control (Figure 9). Application of MS222 reduced activity to $0.24 \pm 0.19\%$ of control. Our one sample t-test revealed that the percent in right parietal nerve activity after MS222 compared to control was statistically significant ($p<0.0001$, $n=7$). As seen in Figure 8, all but two experiments experienced a 100% decrease in nerve activity. The right parietal nerve activity left over following MS222 treatment in those two experiments did not affect the overall trend. There was

some variation in the frequency of right parietal nerve activity between the control experiments, but these differences did not affect the ability to show the predicted effects of MS222 on right parietal nerve activity in *L. stagnalis*.

3.2 Quinoline dose-dependent effects on right parietal nerve activity in *L. stagnalis*

We analyzed the effects of 1000 nM quinoline (n=10), 100 nM (n=10), and 10 nM (n=10) on right parietal nerve activity in *L. stagnalis*. Extracellular recordings of right parietal nerve activity of *L. stagnalis* and analysis of frequency and percent change of control of right parietal nerve activity revealed that quinoline affected neuronal activity in a dose-dependent manner (Figure 10A-B; Figure 11). The mean frequency of right parietal nerve activity after 1000 nM quinoline treatment was $5.7 \pm 0.5\ s^{-1}$ which was significantly less than control at $6.5 \pm 0.6\ s^{-1}$ ($p=0.032$, preplanned paired sample t-test, n=10). The mean frequency of right parietal nerve activity for lower doses of quinoline was $6.6 \pm 0.5\ s^{-1}$ after 100 nM and $6.1 \pm 0.4\ s^{-1}$ after 10 nM, which was not significantly less than control at $6.1 \pm 0.4\ s^{-1}$ and $6.1 \pm 0.4\ s^{-1}$ respectively ($p=0.61$, n=10; $p=0.76$, n=10 respectively, preplanned paired t-tests).

As there was some variability in frequency of right parietal nerve activity, we also expressed activity in the presence of quinoline as a percentage of the control before application (ERS + vehicle) (Figure 10A). The control represents 100% activity. Right parietal nerve activity in the presence of 1000 nM quinoline decreased to $89.2 \pm 4.3\%$ of control, where this decrease was statistically significant ($p=0.033$, n=10, one sample t-test). The right parietal nerve activity in the presence of 100 nM was $103.9 \pm 4.6\%$ of the control and was $99.9 \pm 3.5\%$ of the control in the presence of 10 nM, but the mean percent of control for these lower doses were not statistically significant ($p=0.41$, n=10 and $p=0.98$, n=10 respectively, one sample t-tests).

3.3 2-Methylquinoline caused a non-significant change in right parietal nerve activity

We next examined and analyzed the effects of 1000 nM 2-methylquinoline (n=10) on right parietal nerve activity of *L. stagnalis* where we determined frequency and percent of control of right parietal nerve activity, which revealed 2-methylquinoline caused a non a significant change in right parietal nerve activity (Figure 12A-B; Figure 13). The mean frequency of nerve activity after 1000 nM 2-methylquinoline was $7.41 \pm 0.3\ s^{-1}$, which was not significantly less than control at $7.9 \pm 0.5\ s^{-1}$ ($p=0.082$, n=10, preplanned paired t-test).

We also expressed right parietal nerve activity in presence of 2-methylquinoline as percentage of the control before application (ERS + vehicle) (Figure 13). The mean percent in right parietal nerve activity after 1000 nM 2-methylquinoline was $94.9 \pm 3.5\%$ of the control. The mean percent in nerve activity after 1000 nM 2-methylquinoline compared to control was not statistically significant ($p=0.18$ n=10, one sample t-test).

4. Discussion

The effects of PACs and synthetic HPACs on electrical activity of excitable cells from various model organisms have been studied, but few studies have investigated the neurobiological effects of anthropogenic HPACs found in the environment. This is therefore the first study to investigate the effects of the HPACs quinoline and 2-methylquinoline on the electrical activity of *L. stagnalis* neurons. Using suction electrode electrophysiology, we confirmed that quinoline dose-dependently affected the right parietal nerve activity of *L. stagnalis* neurons.

We found that the frequency of right parietal nerve activity after 1000 nM quinoline was significantly less than the control ($p=0.032$, $n=10$), but was not significantly lower than the control at the lower doses of 100 nM and 10 nM ($p=0.61$, $n=10$; $p=0.76$, $n=10$ respectively). We found the right parietal nerve activity in the presence of 1000 nM quinoline significantly decreased compared to the control ($p=0.033$, $n=10$) quinoline, but was not significant for 100 nM and 10 nM ($p=0.41$, $n=10$; $p=0.98$, $n=10$ respectively). Together, based on these results, we reject the null hypothesis that quinoline would have no effect on right parietal nerve activity of *L. stagnalis* and favour the alternative hypothesis that it does cause an effect on right parietal nerve activity. The mechanism for how quinoline modulates action potentials of *L. stagnalis* neurons is unknown, but we can conclude with confidence that it is neurotoxic at doses of 1000 nM and higher. Through suction electrode experiments, we first demonstrated that the frequency of right parietal nerve activity after 1000 nM 2-methylquinoline was not significantly less than the control ($p=0.082$, $n=10$). In addition, the mean percent in right parietal nerve activity after 1000 nM 2-methylquinoline compared to control was not statistically significant ($p=0.18$, $n=10$).

Together, based on these results, we fail to reject the null hypothesis that 1000 nM 2-methylquinoline would have no effect on right parietal nerve activity in *L. stagnalis*.

4.1 Effects of quinoline on right parietal nerve activity of *L. stagnalis*

Extracellular recordings are a commonly performed technique in electrophysiology (Cámera et al. 2020). They allow researchers to record the electrical activity of excitable cells, mainly in the form of action potentials from single or many firing neurons over a period (Cámera et al. 2020). Data such as frequency of "events" or amplitude of an event can be extracted from these recordings and, if a molecule were to modulate action potentials, changes in frequency or the amplitude of events would be observed. Our results suggest quinoline dose dependently reduced the frequency of action potentials in the right parietal nerve activity of *L. stagnalis* neurons.

The mean frequency of right parietal nerve activity after 1000 nM quinoline treatment was significantly less than the control, although the decrease was modest (11.79%). This is consistent with the findings that phenanthrene, a compound structurally similar to quinoline, dose dependently (5 μM and 25 μM) modulated action potentials in mackerel and yellowfin cardiomyocytes by prolonging action potential duration which in turn decreases the firing rate of these cells (Brett et al. 2017; Grider et al. 2023). Interestingly, by contrast, phenanthrene dose-dependently (0.3 μM, 1μM, 10 μM and 30 μM) modulated action potentials in cardiomyocytes of rainbow trout. However, the action potential duration was shortened, which in turn would increase the firing rate of these cells (Vehniäinen et al. 2019; Grider et al. 2023). These findings on PACs effects and our results with quinoline show they modulated action potentials, but the phenotypes from exposure differ between species. As cardiomyocytes and neurons both express

voltage-gated ion channels, the results from these studies can be compared with ours. It is important to note that concentrations used in these two studies are magnitudes of order higher than the concentrations we used in our study. Our maximum dose was 1000 nM because we limited it to values we might expect to observe at contaminated sites (Vitharana et al. 2024). Furthermore, it might not be practical to test concentrations of a magnitude higher than 1000 nM as those would be concentrations organisms would most likely never encounter.

Our results are consistent with other studies on the neurobiological effects of quinoline derivatives on the electrical activity of snail neurons (Walden and Speckmann 1981; Hermann and Gorman 1984). Quinine dose-dependently (10-100 μM) modulated action potentials in Burgundy snail (*Helix pomatia*) neurons, reducing amplitude and increasing action potential duration (Walden and Speckmann 1981). In addition, 50 μM quinidine modulated action potentials in California sea hare (*Aplysia californica*) by decreasing the action potentials rate of rise and prolonged its duration (Hermann and Gorman 1984). Both studies demonstrate the quinoline derivatives quinine and quinidine modulate the electrical excitability of snail neurons, consistent with our 1000 nM quinoline results. However, the HPAC concentrations those researchers used were much greater than the concentrations used in our study. Most prior research has focused on the neurobiological effects of PACs and synthetic HPACs used in the pharmaceutical industry, and our study provides novel insight into the knowledge gap surrounding the potential neurobiological effects of quinoline.

4.2 Effect of 2-methylquinoline on right parietal nerve activity of *L. stagnalis*

Our results suggest that 1000 nM 2-methylquinoline had no significant effect on right parietal nerve activity of *L. stagnalis* neurons. The frequency of right parietal nerve activity after 1000 nM 2-mehtylquinoline and the percent in activity after 2-methylquinoline compared to

control were not statistically significant. Although we investigated only one concentration, because there was no significant difference at 1000 nM compared to the control, we would not expect there to be a difference at lower concentrations. Based on these results, we rejected our hypothesis that 2-methylquinoline would affect the electrical activity of *L. stagnalis* neurons.

Although, 2-methylquinoline's effect on the electrical activity of excitable cells had not been previously investigated, our results were unlike previous literature investigating effects of other quinoline derivatives such as quinidine and quinine on snail neurons (Walden and Speckmann 1981; Hermann and Gorman 1984). Both studies found 50 μM quinidine and quinine (10-100 μM) modulated the electrical excitability of neurons from California sea hare (*Aplysia californica*) and Burgundy snail (*Helix pomatia*). However, these studies used concentrations well above the concentration used in our study.

The concentration of 2-methylquinoline used in our study was chosen based on known concentrations of 2-methylquinoline in the environment (Vitharana et al. 2024). 1000 nM is greater than the concentrations of 2-methylquinoline found in sediment in the Great Lakes (44 nM - 400 nM) but, due to its potential bioaccumlative nature, tissue concentrations in some aquatic organisms such as yellow perch (*Perca flavescens*) from contaminated sites on Lake Erie had tissue concentrations near 1300 nM (Vitharana et al. 2024; Vitharana et al., 2025, unpublished data). Therefore, our results suggest that 2-methylquinoline at 1000 nM, an environmentally relevant concentration, may not be neurotoxic. Organisms can be exposed to 2-methylquinoline concentrations in the environment higher than 1000 nM, and we could potentially study higher doses, but environmental relevance is limited. Further investigation is therefore needed before conclusions can be made about its neurotoxicity.

4.3 Is quinoline a molecule of concern for acute neurological effects?

Increasing environmental concentrations of quinoline from anthropogenic sources, and its persistent nature, represent a concerning trend, as our results demonstrate that 1000 nM quinoline caused a significant decrease in mean frequency of right parietal nerve activity of *L. stagnalis* neurons ($p<0.05$ $n=10$). However, this decrease was modest (11.79%). The concentration of quinoline we used was close to concentrations (within an order of magnitude) found in sediment in the Great Lakes which ranged from 44 nM to 644 nM (Vitharana et al., 2025, unpublished data). Although, there are reports with conflicting stances on whether quinoline is bioaccumulative or not, very recent data shows concentrations found in Lake Erie walleye (*Sander vitreus*) were as high as 1952 nM, two-fold higher than the concentration used in our study (Vitharana et al., 2025, unpublished data). The concentration used in our study is thus highly relevant environmentally. Our results suggest that because many aquatic organisms are exposed to higher concentrations of quinoline we should consider studying higher concentrations, where possible adverse neurobiological effects of quinoline are potentially worse. In addition, for better comparison with previous literature who used higher concentrations, future studies could study quinoline concentrations of 10 000 nm and 100 000 nM. Although this would be a concentration way higher than what an organism would experience, it would allow for a better comparison with previous literature.

Our study, and others investigating PACs and synthetic HPACs, have looked at the acute effects of quinoline and its derivatives on the health of organisms. However, a next step would be to investigate the long-term effects of chronic exposure to quinoline and its derivatives on the functions and development of the nervous system. The bioaccumulative nature of quinoline is debated, but very recent data suggests there is evidence various fishes and aquatic invertebrates

have higher concentrations of quinoline than what is found in the environment, and chronic exposure could therefore have long-term effects on the nervous system and neurodevelopment (Environment and Climate Change 2011; Vitharana et al., 2025, unpublished data).

With the increase in the presence of quinoline and its derivatives in the environment and their persistent behaviour, humans could be exposed to quinoline for longer than the ten-minute *L. stagnalis* exposure in this experiment. An epidemiological study found that prenatal exposure to PACs on the neurodevelopment of inner-city children in New York where they found children, having been exposed to the highest levels of PACs in polluted air (36.47 ng/m3), at three years of age scored the lowest on the mental development index (Perera et al. 2006). This provides some correlative evidence that chronic exposure to numerous PACs may disrupt neurodevelopment. HPACs are related to PAC, and it is therefore not unreasonable to predict similar effects could result from chronic exposure to HPACs. However, the risks of chronic exposure to these contaminants remain largely unknown.

4.4 Limitations and Future directions

A limitation of our study is that for our analysis of electrical activity we grouped the "events" of our extracellular recordings together as "right parietal nerve activity", without further looking into the spike characteristics of these "events", a process known as spike sorting (Rey et al. 2015). In brief, spike sorting is a technique that allows for spikes to be grouped together based on similar characteristics, where groups of similar spikes correspond to a single or group of neurons (Rey et al. 2015). Although our method is successful at demonstrating the overall effects of quinoline and 2-methylquinoline on right parietal nerve activity of *L. stagnalis* neurons, notice the large, medium and small spikes in Figure 5, with spike sorting it would allow for a more in-

depth analysis into the individual firing characteristics of single or a group of neurons since different neurons respond to external stimuli differently (Rey et al. 2015). This could provide important data into potential mechanisms explaining the modulation of action potentials of *L. stagnalis* neurons by quinoline and its derivatives. To better understand the potential mechanisms explaining the modulation of action potentials of *L. stagnalis* neurons by quinoline and its derivatives, future studies could use patch clamp electrophysiology. This is the gold-standard technique for electrophysiological analysis as it allows for the measurement of single neurons and specific ion currents. A caveat of this technique is that it is very technical and requires high level of training. It is also a low throughput technique in comparison to suction electrode experiments which are meant to be relatively simple and fast.

It would be interesting to understand the potential mechanisms explaining quinoline's effects on right parietal nerve activity of *L. stagnalis* neurons, particularly as they have well conserved ion channels shared between organisms, meaning results are relevant to mammals - especially humans. However, future studies should investigate quinoline's neurobiological effects on electrical excitability of mammalian neurons. In addition, with environmental concentrations of quinoline and its derivatives increasing, their persistent nature and evidence of bioaccumulation in animal tissue, future studies should investigate the effects of quinoline on neurodevelopment because of long-term exposure. It is important to note these chemicals do not persist in the environment in isolation and occur in mixtures with other HPACs. Therefore, effects on organisms from this mixture could be even worse.

Our study is the first study demonstrating the neurotoxic behaviour of quinoline on *L. stagnalis* neurons, providing evidence on the importance of monitoring and demonstrates the utility of suction electrode recordings as an electrophysiology technique to evaluate acute

neurotoxicity of environmental contaminants. This technique could be used to study the adverse effects of many HPACs, which would be essential since these chemicals persist in the environment in mixtures. Future studies on HPACs effects on neurodevelopment from long-term exposure in mammals would provide insight into the importance of monitoring them, provide evidence for stricter regulations on HPACs, and further demonstrate their risk to humans.

Literature Cited

Abdel-Shafy HI, Mansour MSM (2016) A review on polycyclic aromatic hydrocarbons: Source, environmental impact, effect on human health and remediation. Egyptian Journal of Petroleum 25:107–123.

Amorim J, Abreu I, Rodrigues P, Peixoto D, Pinheiro C, Saraiva A, Carvalho AP, Guimarães L, Oliva-Teles L (2019) Lymnaea stagnalis as a freshwater model invertebrate for ecotoxicological studies. Science of The Total Environment 669:11–28.

Andersson H, Lindqvist E, Westerholm R, Grägg K, Almén J, Olson L (1998) Neurotoxic Effects of Fractionated Diesel Exhausts Following Microinjections in Rat Hippocampus and Striatum. Environmental Research 76:41–51.

Andersson JT, Achten C (2015) Time to Say Goodbye to the 16 EPA PAHs? Toward an Up-to-Date Use of PACs for Environmental Purposes. Polycyclic Aromatic Compounds 35:330–354.

Arnot JA, Gobas FA (2006) A review of bioconcentration factor (BCF) and bioaccumulation factor (BAF) assessments for organic chemicals in aquatic organisms. Environmental Reviews 14:257–297.

Beekharry CC, Zhu GZ, Magoski NS (2015) Role for electrical synapses in shaping the output of coupled peptidergic neurons from Lymnaea. Brain Research 1603:8–21.

Benjamin PR (2008) Lymnaea. Scholarpedia. Available at http://www.scholarpedia.org/article/Lymnaea [Accessed September 2, 2024].

Berthiaume A, Galarneau E, Marson G (2021) Polycyclic aromatic compounds (PACs) in the Canadian environment: Sources and emissions. Environmental Pollution 269:116008.

Brette F, Shiels HA, Galli GLJ, Cros C, Incardona JP, Scholz NL, Block BA (2017) A Novel Cardiotoxic Mechanism for a Pervasive Global Pollutant. Scientific Reports 7:41476.

Brinkmann M, Blenkle H, Salowsky H, Bluhm K, Schiwy S, Tiehm A, Hollert H (2014) Genotoxicity of Heterocyclic PAHs in the Micronucleus Assay with the Fish Liver Cell Line RTL-W1 Pant AB, ed. Public Library of Science ONE 9:e85692.

Cámera A, Belluscio MA, Tomsic D (2020) Multielectrode Recordings From Identified Neurons Involved in Visually Elicited Escape Behavior. Frontiers in Behavioural Neuroscience 14:592309.

Canada Environment and Climate Change (2011) Screening Assessment. Available at: https://www.canada.ca/en/environment-climate-change/services/evaluating-existing-substances/screening-assessment-4.html [Accessed September 1, 2024].

Canada Health (2010) Quinoline. Available at: https://www.canada.ca/en/health-canada/services/chemical-substances/fact-sheets/chemicals-glance/quinoline.html [Accessed September 1, 2024].

Chen H-Y, Preston MR (1998) Azaarenes in the Aerosol of an Urban Atmosphere. Environmental Science and Technology 32:577–583.

Chuang JC, Mack GA, Kuhlman MR, Wilson NK (1991) Polycyclic aromatic hydrocarbons and their derivatives in indoor and outdoor air in an eight-home study. Atmospheric Environment Part B Urban Atmosphere 25:369–380.

Do S-H (2013) Magnesium: a versatile drug for anesthesiologists. Korean Journal of Anesthesiology 65:4.

Ducouret P (1976) The effect of quinidine on membrane electrical activity in frog auricular fibres studied by current and voltage clamp. British Journal of Pharmacology 57:163–184.

Fowler MG, Brooks PW, Northcott M, King MWG, Barker JF, Snowdon LR (1993) Preliminary results from a field experiment investigating the fate of some creosote components in a natural aquifer. In Advances of Organic Chemistry (Oygard K, ed), pp641-649. Stavanger: English Scientific.

Furlong ET, Carpenter R (1982) Azaarenes in Puget sound sediments. Geochimica et Cosmochimica Acta 46:1385-1396.

Grider MH, Jessu R, Kabir R (2025) Physiology, Action Potential. In: StatPearls. Treasure Island (FL): StatPearls Publishing. Available at: http://www.ncbi.nlm.nih.gov/books/NBK538143/ [Accessed March 21, 2025].

Hasegawa R, Furukawa F, Toyoda K, Sato H, Imaida K, Takahashi M (1989) Sequential analysis of quinoline-induced hepatic hemangioendothelioma development in rats. Carcinogenesis 10:711–716.

Hermann A, Gorman AL (1984) Action of quinidine on ionic currents of molluscan pacemaker neurons. The Journal of general physiology 83:919–940.

Kimbrough K, Jacob A, Regan S, Davenport E, Edwards M, Leight AK, Freitag A, Rider M, Johnson WE (2021) Characterization of polycyclic aromatic hydrocarbons in the Great Lakes Basin using *dreissenid* mussels. Environmental and Monitoring Assessment 193:833.

Kompella SN, Brette F, Hancox JC, Shiels HA (2021) Phenanthrene impacts zebrafish cardiomyocyte excitability by inhibiting IKr and shortening action potential duration. Journal of General Physiology 153:e202012733.

LaVoie EJ, Shigematsu A, Adams EA, Rigotty J, Hoffmann D (1984) Tumor-initiating activity of quinoline and methylated quinolines on the skin of SENCAR mice. Cancer Letters 22:269–273.

Lucas J, Percelay I, Larcher T, Lefrançois C (2016) Effects of pyrolytic and petrogenic polycyclic aromatic hydrocarbons on swimming and metabolic performance of zebrafish contaminated by ingestion. Ecotoxicology and Environmental Safety 132:145–152.

Luongo G, Thorsén G, Östman C (2014) Quinolines in clothing textiles—a source of human exposure and wastewater pollution? Analytical and Bioanalytical Chemistry 406:2747–2756.

Marvin CH, Berthiaume A, Burniston DA, Chibwe L, Dove A, Evans M, Hewitt LM, Hodson PV, Muir DCG, Parrott J, Thomas PJ, Tomy GT (2021) Polycyclic aromatic compounds in the Canadian Environment: Aquatic and terrestrial environments. Environmental Pollution 285:117442.

Minnesota Polution Control Agency (2011) Annual Monitoring Report for 2011. Available at: https://www.pca.state.mn.us/search [Accessed September 2, 2024].

Nawrath H, Eckel L (1979) Electrophysiological study of human ventricular heart muscle treated with quinidine: interaction with isoprenaline. Journal of Cardiovascular Pharmacology 1: 415-425.

Neuwoehner J, Reineke A-K, Hollender J, Eisentraeger A (2009) Ecotoxicity of quinoline and hydroxylated derivatives and their occurrence in groundwater of a tar-contaminated field site. Ecotoxicology and Environmental Safety 72:819–827.

Nezlin L, Voronezhskaya E (1997) GABA-immunoreactive neurones and interactions of GABA with serotonin and FMRFamide in a peripheral sensory ganglion of the pond snail Lymnaea stagnalis. Brain Research 772:217–225.

Novack L, Brodie BB (1950) Quinoline and its transformation products found in urine. Journal of Biological Chemistry 187:787–792.

Peddinghaus S, Brinkmann M, Bluhm K, Sagner A, Hinger G, Braunbeck T, Eisenträger A, Tiehm A, Hollert H, Keiter SH (2012) Quantitative assessment of the embryotoxic potential of NSO-heterocyclic compounds using zebrafish (Danio rerio). Reproductive Toxicology 33:224–232.

Perera FP, Rauh V, Whyatt RM, Tsai W-Y, Tang D, Diaz D, Hoepner L, Barr D, Tu Y-H, Camann D, Kinney P (2006) Effect of Prenatal Exposure to Airborne Polycyclic Aromatic Hydrocarbonson Neurodevelopment in the First 3 Years of Life among Inner-City Children. Environmental Health Perspectives 114:1287–1292.

Reign G, McMahon H, Ishizaki M, Ohara T, Shimane K, Esumi Y, Green C, Tyson C, Ninomiya S (1996) Cytochrome P450 species involved in the metabolism of quinoline. Carcinogeenesis 17:1989–1996.

Rey HG, Pedreira C, Quian Quiroga R (2015) Past, present and future of spike sorting techniques. Brain Research Bulletin 119:106–117.

Saunders CR, Das SK, Ramesh A, Shockley DC, Mukherjee S (2006) Benzo(a)pyrene-induced acute neurotoxicity in the F-344 rat: role of oxidative stress. Journal of Applied Toxicology 26:427–438.

Smith RS, Kenny CJ, Ganesh V, Jang A, Borges-Monroy R, Partlow JN, Hill RS, Shin T, Chen AY, Doan RN, Anttonen AK, Ignatius J, Medne L, Bönnemann CG, Hecht JL, Salonen O, Barkovich AJ, Poduri A, Wilke M … Lehtinen MK (2018) Sodium channel SCN3A (NaV1.3) regulation of human cerebral cortical folding and oral motor development. Neuron 99:905-913.e7.

Southworth GR, Keffer CC, Beauchamp JJ (1980) Potential and realized bioconcentration. A comparison of observed and predicted bioconcentration of azaarenes in the fathead minnow (Pimephales promelas). Environmental Science and Technology 14:1529–1531.

Suzuki T, Miyata Y, Saeki K, Kawazoe Y, Hayashi M, Sofuni T (1998) *In vivo* mutagenesis by the hepatocarcinogen quinoline in the lacZ transgenic mouse: evidence for its *in vivo* genotoxicity. Mutation Research/Genetic Toxicology and Environmental Mutagenesis 412:161–166.

Sverdrup LE, De Vaufleury A, Hartnik T, Hagen SB, Loibner AP, Jensen J (2006) Effects and uptake of polycyclic aromatic compounds in snails (*Helix aspersa*). Environmental Toxicology and Chemistry 25:1941–1945.

TCI AMERICA (2024) 2-Methylquinoline 91-63-4 | TCI AMERICA. Available at: https://www.tcichemicals.com/MX/en/p/Q0005 [Accessed September 5, 2024].

TCI AMERICA (2024) Search phenanthrene | TCI AMERICA. Available at: https://www.tcichemicals.com/MX/en/search/?text=phenanthrene [Accessed September 5, 2024].

TCI AMERICA (2024) Search quinoline | TCI AMERICA. Available at: https://www.tcichemicals.com/MX/en/search/?text=quinoline [Accessed September 5, 2024].

U.S. Environmental Protection Agency (2001) Toxicological review of quinoline. Available at: https://iris.epa.gov/static/pdfs/1004tr.pdf [Accessed December 1, 2024].

U.S. Environmental Protection Agency (1985) Health and environmental effects profile for quinoline. Available at:

https://ntrl.ntis.gov/NTRL/dashboard/searchResults.xhtml?searchQuery=PB88183124&starDB=GRAHIST [Accessed December 1, 2024].

Vehniäinen E-R, Haverinen J, Vornanen M (2019) Polycyclic Aromatic Hydrocarbons Phenanthrene and Retene Modify the Action Potential via Multiple Ion Currents in Rainbow Trout Oncorhynchus mykiss Cardiac Myocytes. Environmental Toxicology and Chemistry 38:2145–2153.

Vitharana NN, Halldorson T, Xia Z, Francisco O, Marvin C, Thomas PJ, Liebzeit E, Lucas A-M, Moradi V, Tomy GT (2024) A validated approach for analysis of heterocyclic aromatic compounds in sediment samples. Journal of Chromatography A 1718:464723.

Walden J, Speckmann E-J (1981) Effects of quinine on membrane potential and membrane currents in identified neurons of Helix pomatia. Neuroscience Letters 27:139–143.

Wang CM, Parker CH (1980) Reassessment of the electrophysiological effects of the antiarrhythmic agent quinidine in canine Purkinje fibers. Life Sciences 27:663–670.

Wang Z, Yang C, Parrott JL, Frank RA, Yang Z, Brown CE, Hollebone BP, Landriault M, Fieldhouse B, Liu Y, Zhang G, Hewitt LM (2014) Forensic source differentiation of petrogenic, pyrogenic, and biogenic hydrocarbons in Canadian oil sands environmental samples. Journal of Hazardous Materials 271:166–177.

Wyttenbach RA, Johnson BR, Hoy RR (2022). Snail ganglia: Control of feeding (draft). *Crawdad: An Online Lab Manual for Neurophysiology*. https://nbb.emory.edu/wyttenbach/crawdad/12.SnailGanglia.html [Accessed September 2, 2024].

Zhao Y-Q, Li X, Guo H-Y, Shen Q-K, Quan Z-S, Luan T (2023) Application of Quinoline Ring in Structural Modification of Natural Products. Molecules 28:6478.

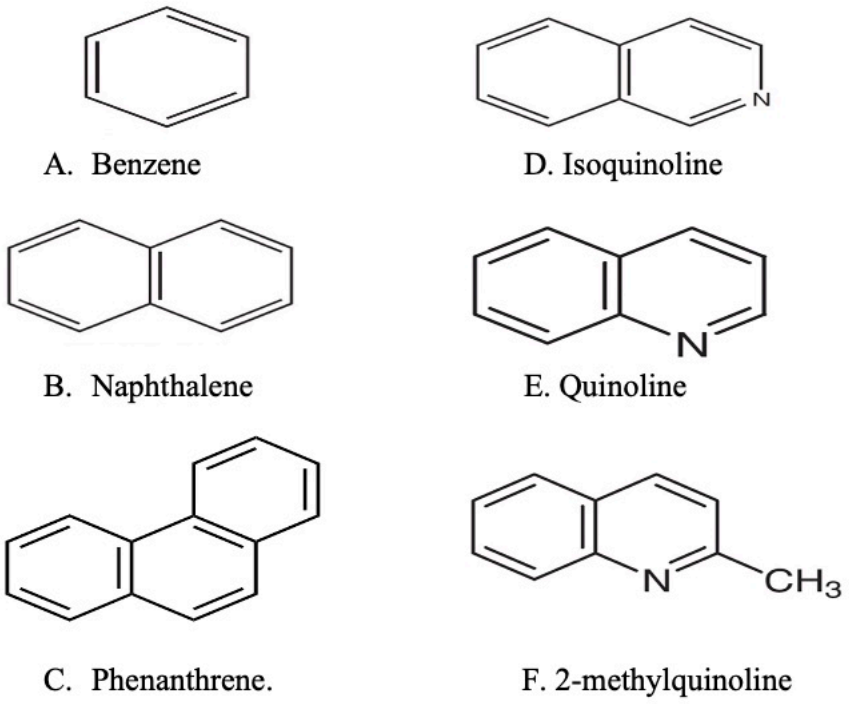

Figure 1. Chemical structures of assorted aromatic compounds. A. chemical structure of the monoaromatic benzene. B-C. chemical structure of the polycyclic aromatic compound's naphthalene, and phenanthrene. E-F. chemical structure of the hetero-polycyclic aromatic compounds isoquinoline, quinoline, and 2-methylquinoline (Boersma 2009; TCI America 2024).

(A) (B)

Figure 2. Anatomy of *Lymnaea stagnalis*. (A) Whole body diagram of *Lymnaea stagnalis* illustrating the location of the CNS and heart (Benjamin 2008) (B) Picture of the *Lymnaea stagnalis* central nervous system (CNS) pinned dorsal side up. Labels showing the location of the right parietal ganglion (RPG), buccal ganglia and the right internal nerve of the right parietal ganglion.

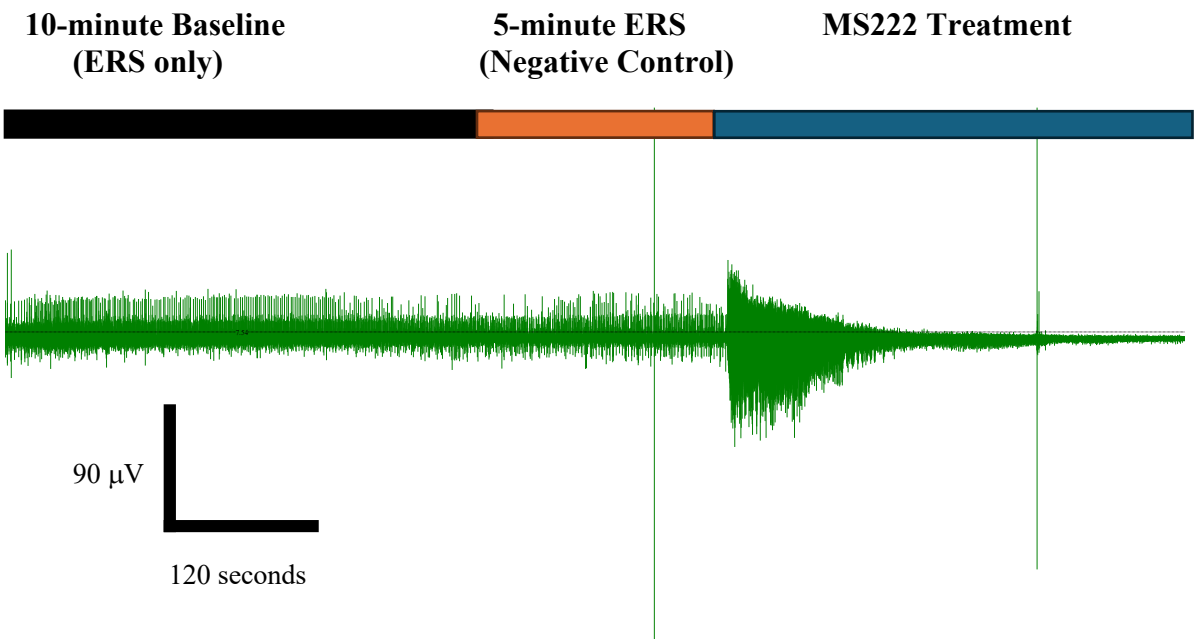

Figure 3. A sample extracellular recording of the right parietal nerve activity of *Lymnaea stagnalis* neurons during a suction electrode experiment. The experiment is comprised of a ten-minute ERS control (black), five-minute ERS negative control (orange), and ten-minute MS222 treatment (38.3 mM). The horizontal cursor represents the threshold of electrical events. The whole recording was 1535 seconds.

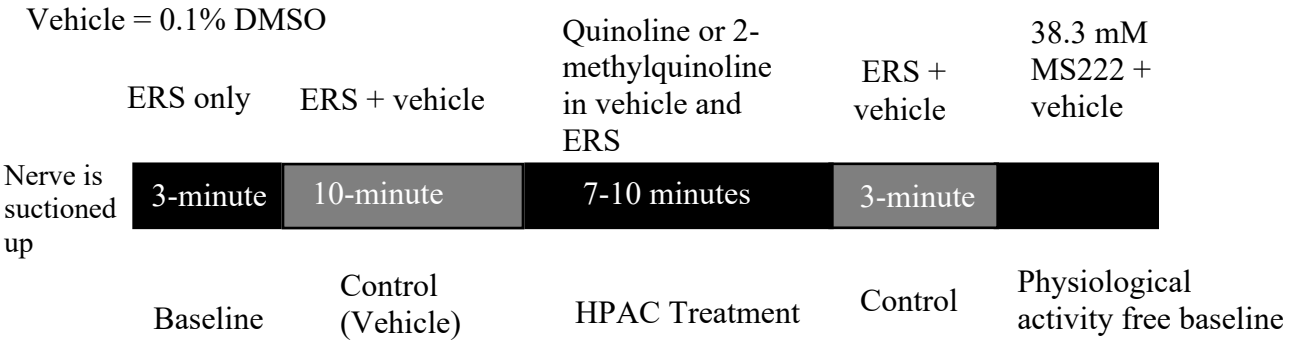

Figure 4. A flowchart outlining the protocol for the suction electrode experiment and its timing for HPAC (quinoline and 2-methylquinoline) treatments and controls. Vehicle is 0.1% DMSO.

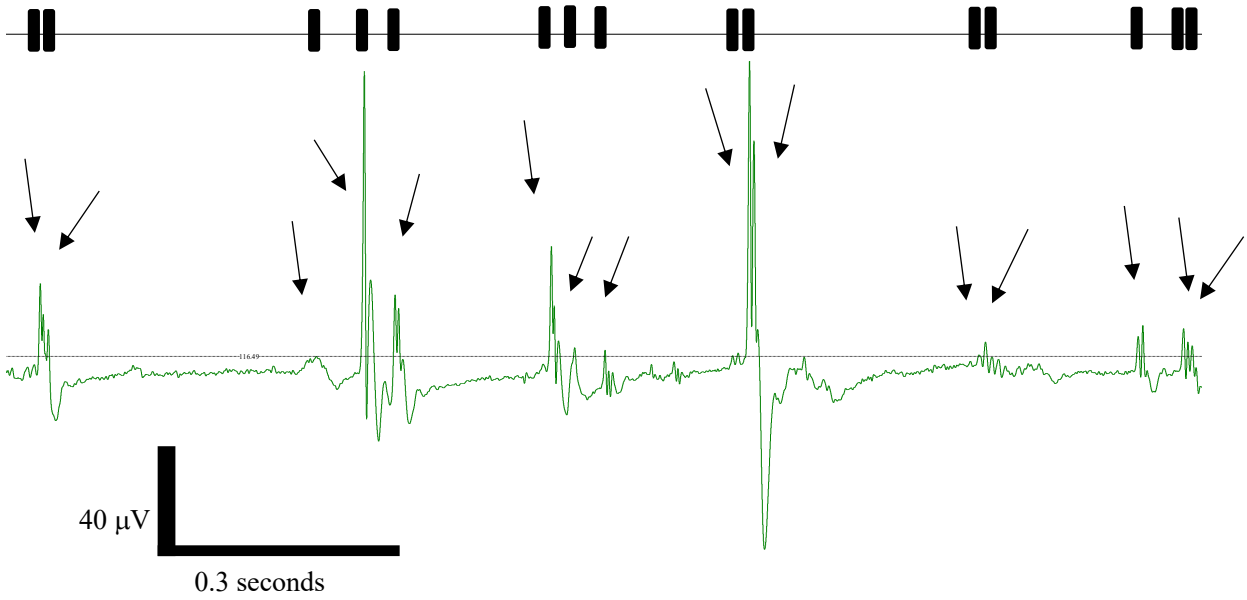

Figure 5. Inset of a sample extracellular recording of right parietal nerve activity of *Lymnaea stagnalis* neurons. The method of measuring the frequency of right parietal nerve activity is displayed. Events that cross the determined threshold (116.49 µV) are deemed electrical activity and used for calculating the frequency. The arrows show each time an event crosses the threshold. The whole recording was 1.4 seconds.

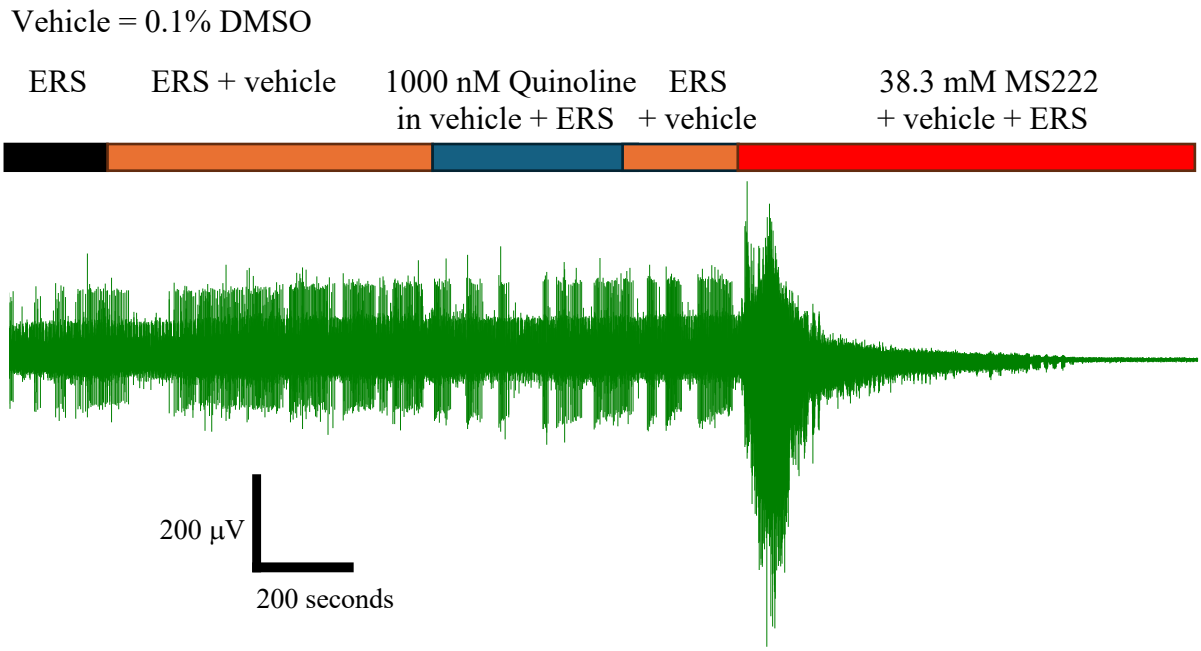

Figure 6. A sample extracellular recording of right parietal nerve activity of *Lymnaea stagnalis* neurons during the HPAC suction electrode experiment. The experiment is comprised of a 3-minute ERS control (black), 15-minute ERS + vehicle (0.1% DMSO) control (orange), 1000 nM Quinoline in vehicle (0.1% DMSO) + ERS (blue), followed by a 38.3 mM MS222 treatment in vehicle (0.1% DMSO) (red). The entire recording was 2180 seconds.

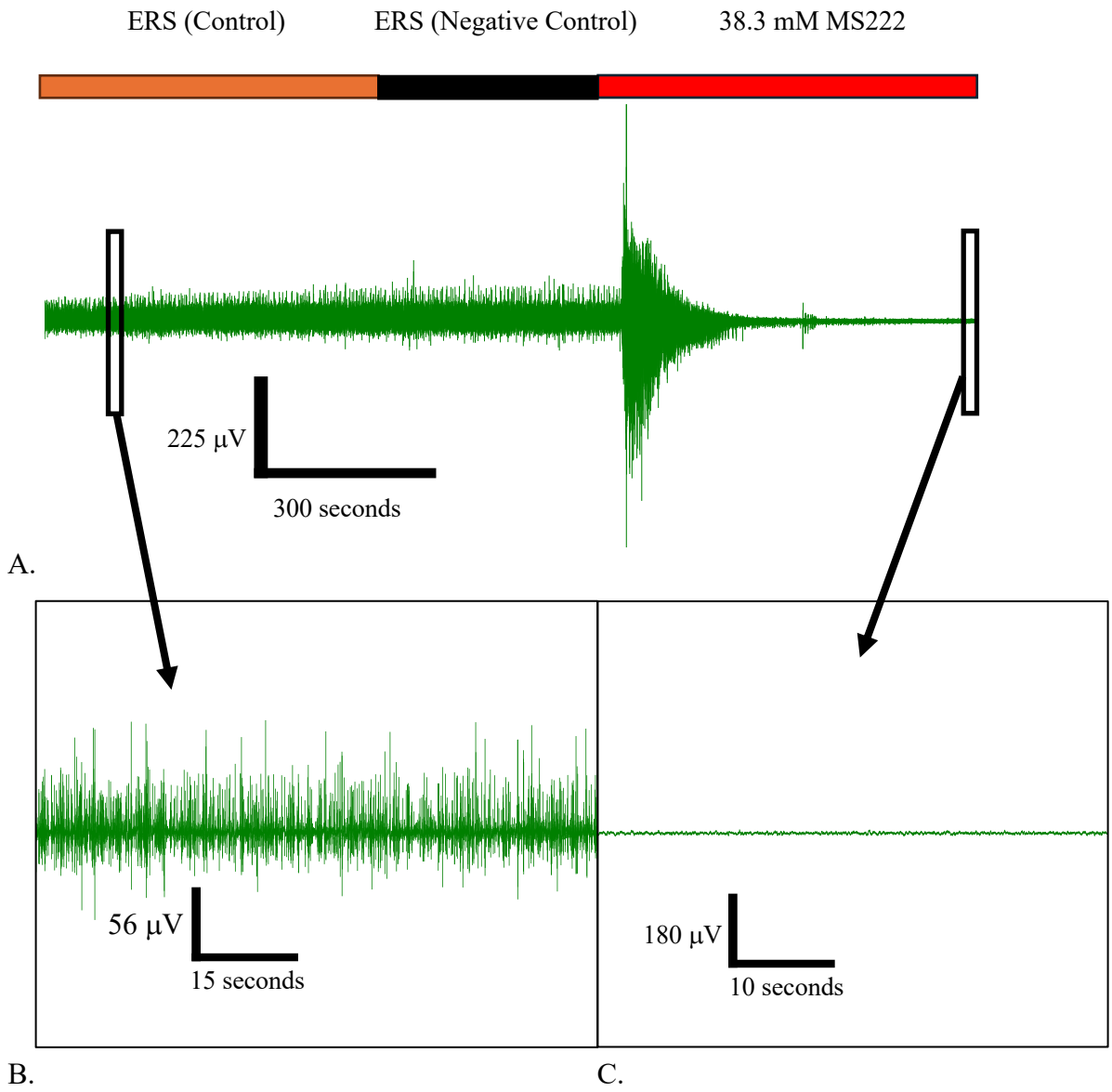

Figure 7. Sample extracellular recordings of right parietal nerve activity of *Lymnaea stagnalis* neurons before and after application of 38.3 mM MS222. (A). A sample extracellular recording of right parietal nerve activity of *Lymnaea stagnalis* neurons during a suction electrode experiment. The experiment is comprised of a 10-minute ERS control (orange), 5-minute ERS negative control (black), and 10-minute MS222 treatment (38.3 mM) (red). (B) Enlarged recording within the grey box in figure 7A (C). Enlarged recording within the grey box in figure 7A, demonstrating no right parietal nerve activity after MS222 (38.3 mM) treatment. The whole extracellular recording was 1560s.

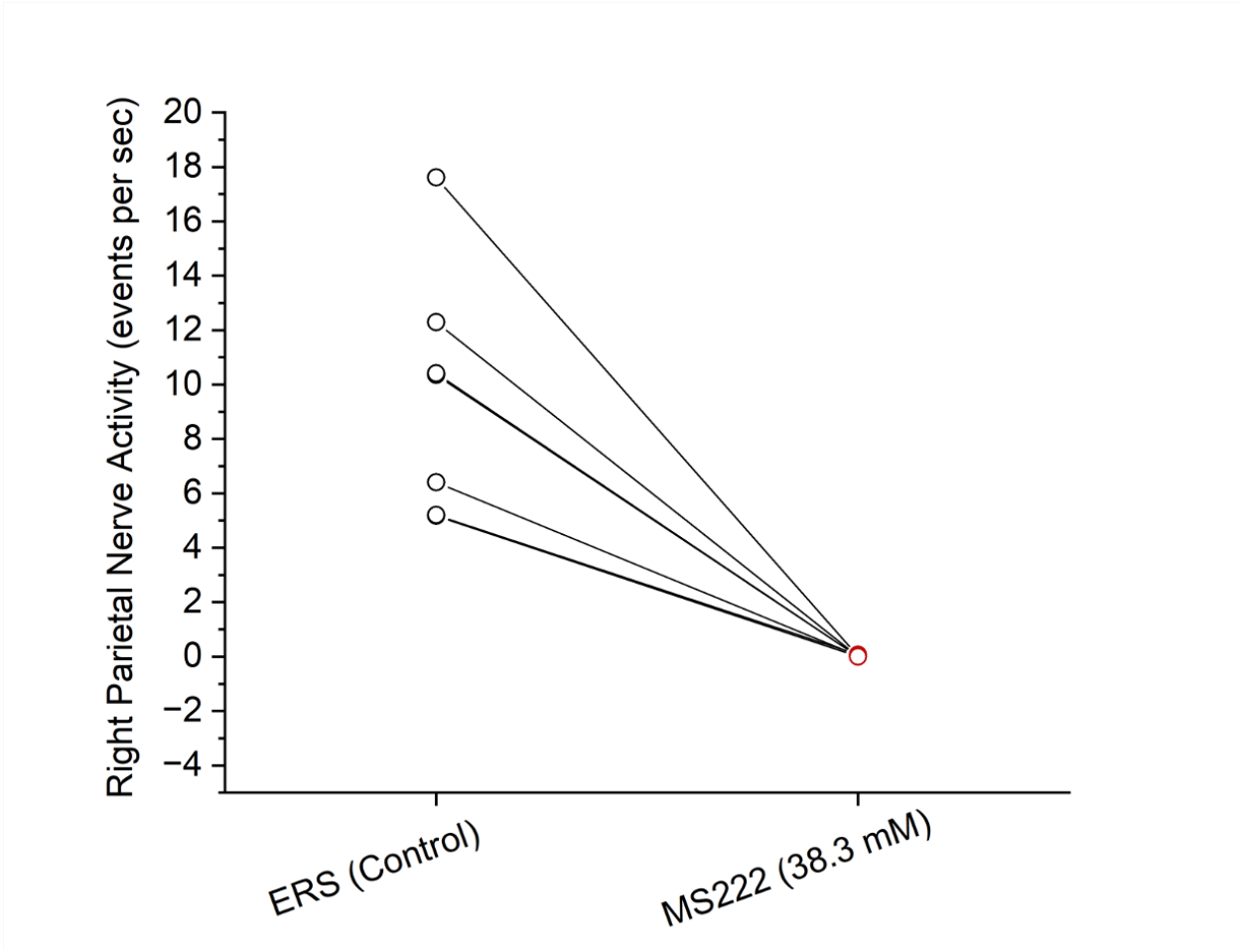

Figure 8. Line series plot comparing frequency (events per sec; s^{-1}) of right parietal nerve activity of *Lymnaea stagnalis* neurons before and after treatment of 38.3 mM MS222. The mean frequency of right parietal nerve activity was significantly different than control (p=0.0013, n=7).

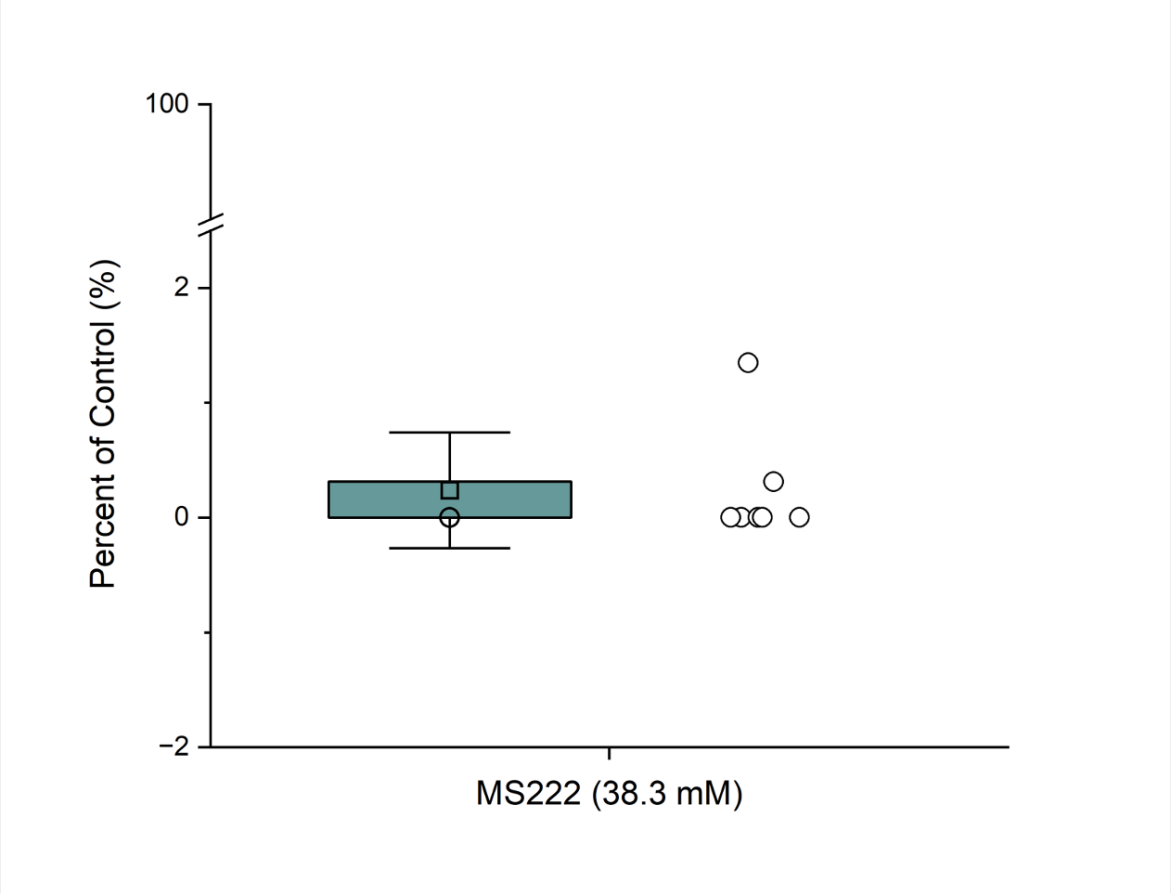

Figure 9. Box plot of right parietal nerve activity of *Lymnaea stagnalis* neurons in the presence of 38.3 mM MS222 as a percentage of control before application of 38.3 mM MS222. The whiskers defined by ± the standard deviation. The box represents the 25th and 75th percentiles. The mini hollow square within the box plot represents the mean, where the hollow circle represents the median of the data. One sample t-test reveals that the mean percent of control after 38.3 mM MS222 treatment was statistically significant ($p<0.0001$, $n=7$).

Figure 10. Quinoline dose-dependently reduced right parietal nerve activity in *Lymnaea stagnalis*. (A) A sample extracellular recording of right parietal nerve activity of *Lymnaea stagnalis* neurons during a suction electrode experiment. The experiment consists of a 3-minute experiment washing over the CNS of *Lymnaea stagnalis* with external recording solution (ERS) (black), then a 10-minute external recording solution containing 0.1% DMSO (orange), then 1000 nM quinoline treatment (blue), 3-minute ERS (purple), and finally washing it over with 38.3 mM MS222 (red). B. Merging of three separate line plots comparing the frequency of right parietal nerve activity after quinoline treatment with that of the control. Our paired sample t-test reveals the mean frequency of right parietal nerve activity (events per sec; s^{-1}) after 1000 nM was significantly different than the control ($p=0.033$ $n=10$), but for 100 nM and 10 nM the frequency was not significantly different than control ($p=0.61$ $n=10$, $p=0.76$ $n=10$ respectively). The entire recording was 2120 seconds.

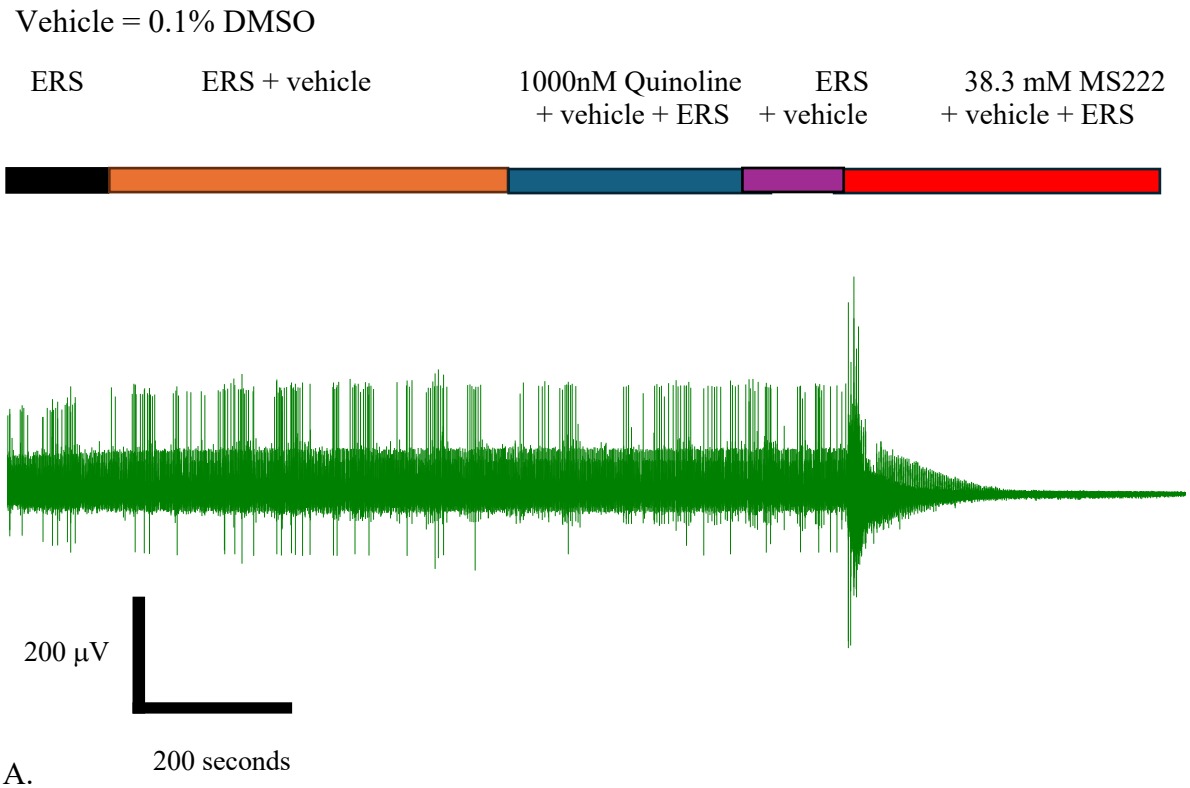
Vehicle = 0.1% DMSO
ERS
ERS + vehicle
1000nM Quinoline
+ vehicle + ERS
ERS
+ vehicle
38.3 mM MS222
+ vehicle + ERS
200 µV
200 seconds

A.

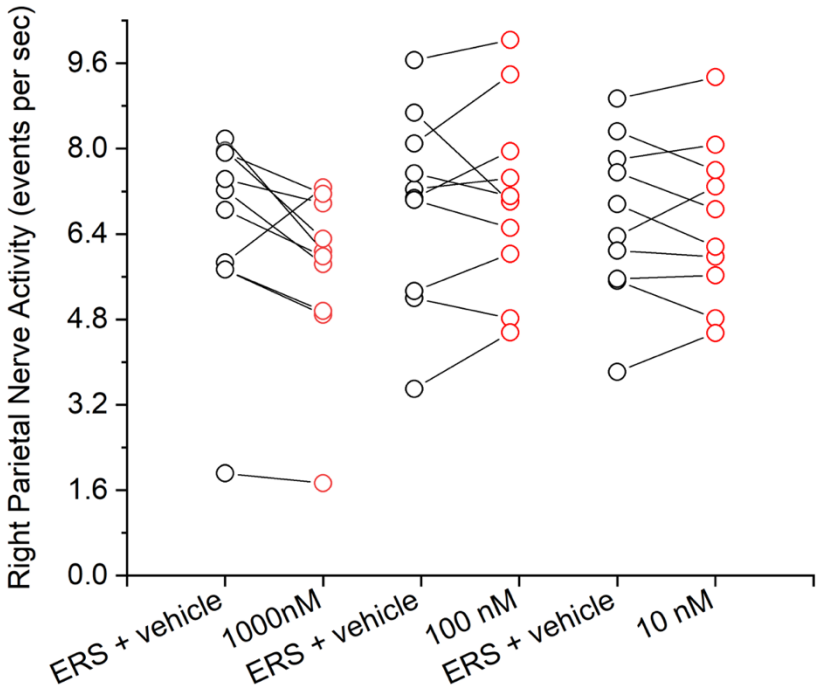
Right Parietal Nerve Activity (events per sec)
9.6
8.0
6.4
4.8
3.2
1.6
0.0
ERS + vehicle
1000nM
ERS + vehicle
100 nM
ERS + vehicle
10 nM

B.

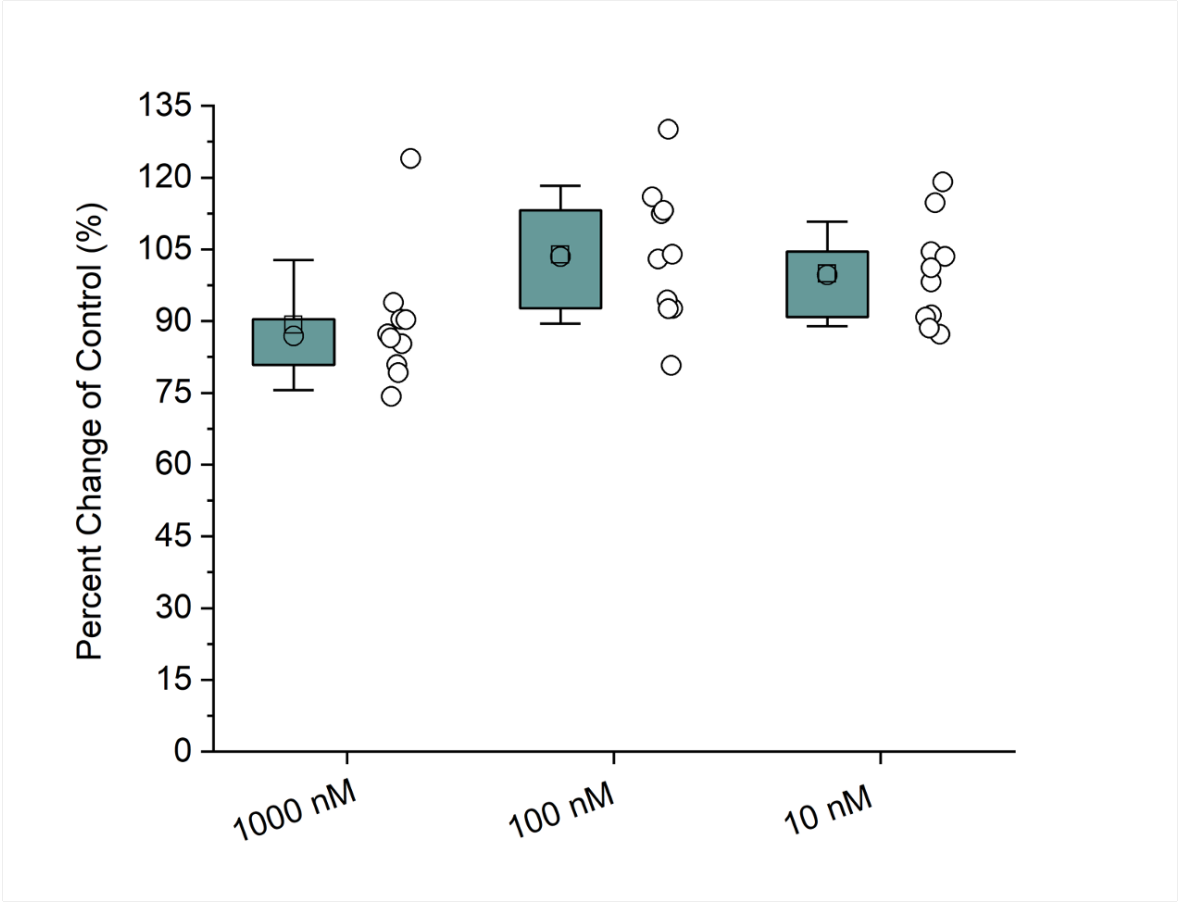

Figure 11. Box plots demonstrating the right parietal nerve activity of *Lymnaea stagnalis* neurons in the presence of quinoline (1000 nM, 100 nM, 10 nM) as a percentage of control before application of quinoline. The whiskers are defined by ± the standard deviation. The box represents the 25th and 75th percentiles. The mini hollow square within the box plot represents the mean, where the hollow circle represents the median of the data. Our one-sample t-test revealed right parietal nerve activity in the presence of 1000 nM quinoline significantly decreased ($p=0.033$ $n=10$), but values were not statistically significant for 100 nM and 10 nM ($p=0.41$ $n=10$, $p=0.98$ $n=10$).

Figure 12. 2-methylquinoline had no significant effect on right parietal nerve activity of *Lymnaea stagnalis* neurons. (A) A sample extracellular recording of right parietal nerve activity of *Lymnaea stagnalis* neurons during the 2-methylquinoline suction electrode experiment. The experiment consists of a 3-minute experiment washing over the CNS of *Lymnaea stagnalis* with external recording solution (ERS) (black), then a 10-minute external recording solution containing 0.1% DMSO (orange), then 1000 nM 2-methylquinoline treatment (blue), 3-minute ERS (purple), and finally washing it over with 38.3 mM MS222 (red). (B) Line series plot comparing the frequency of right parietal nerve activity (events per sec; s^{-1}) before and after 1000 nM 2-methylquinoline. Our paired sample t-test revealed the mean frequency of right parietal nerve activity after 1000 nM 2-methylquinoline treatment was not significantly less than the control ($p=0.082$, $n=10$). The entire recording was 2800 seconds.

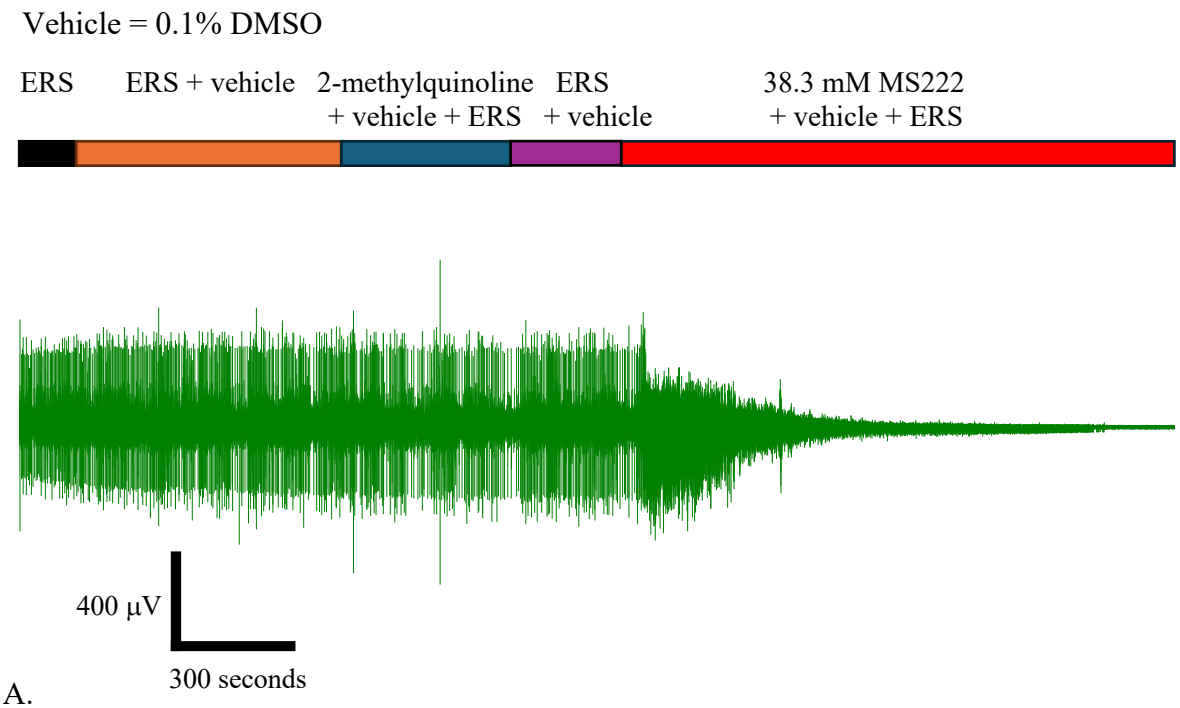
Vehicle = 0.1% DMSO
ERS
ERS + vehicle
2-methylquinoline + vehicle + ERS
ERS + vehicle
38.3 mM MS222 + vehicle + ERS
400 µV
300 seconds

A.

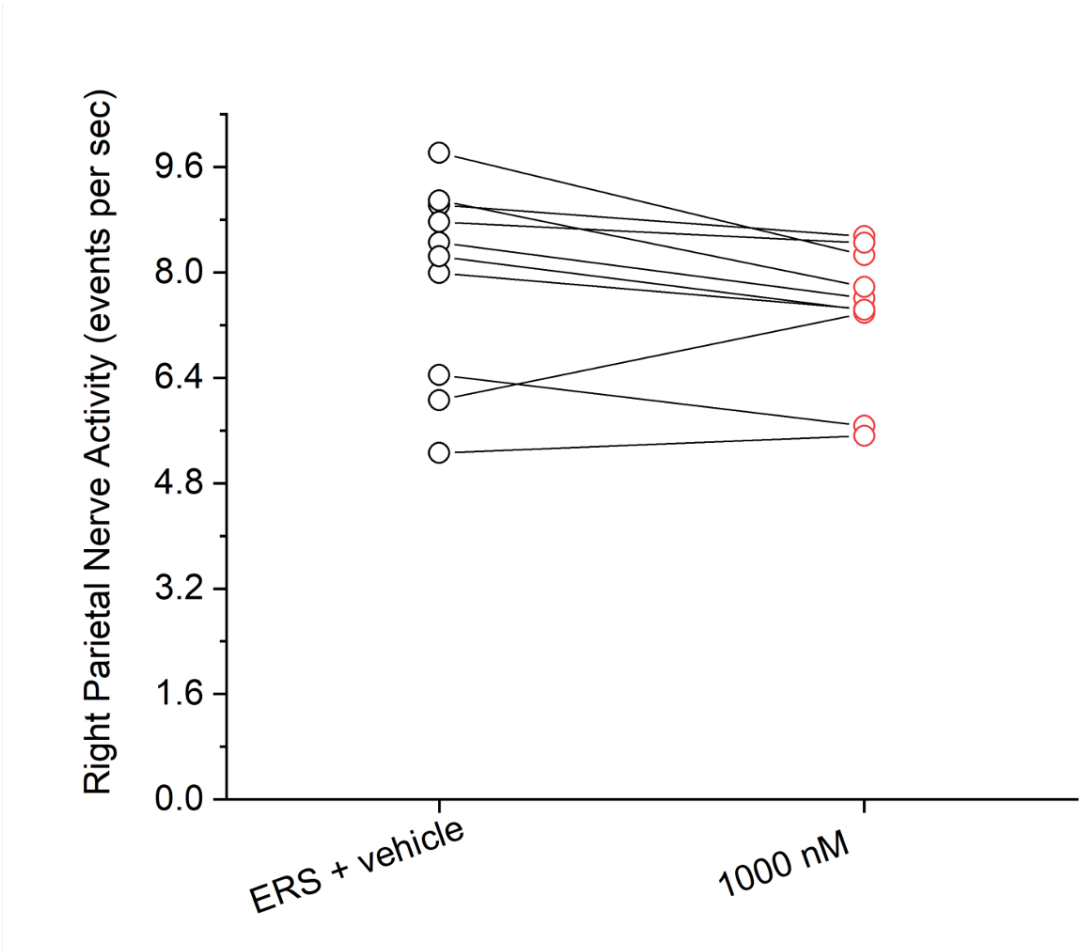
Right Parietal Nerve Activity (events per sec)
9.6
8.0
6.4
4.8
3.2
1.6
0.0
ERS + vehicle
1000 nM

B.

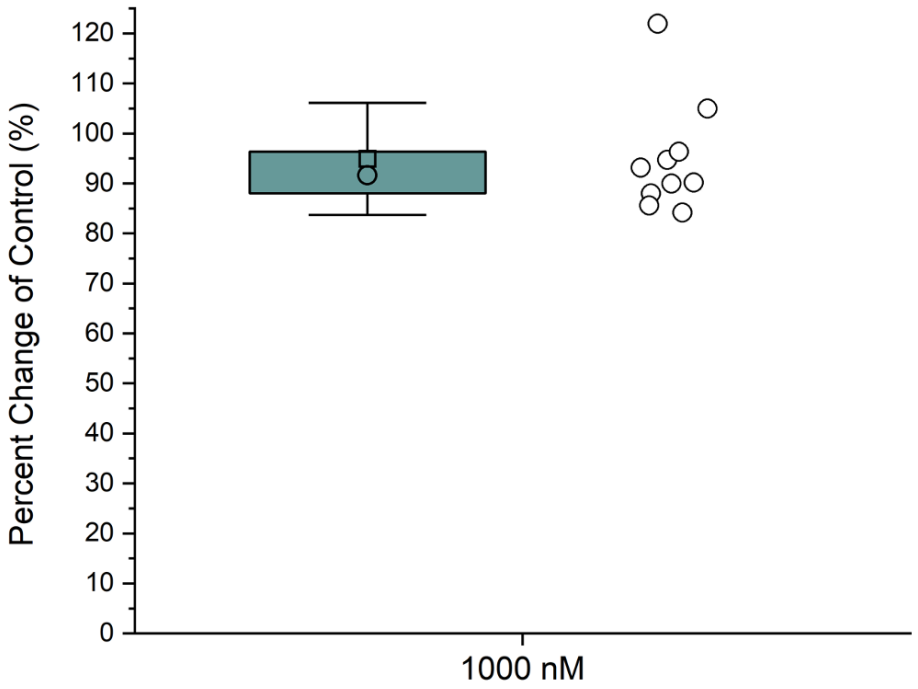

Figure 13. Box plots demonstrating the right parietal nerve activity of *Lymnaea stagnalis* neurons in the presence of 2-methylquinoline as a percentage of control before application of 2-methylquinoline. The whiskers are defined by ± the standard deviation. The box represents the 25th and 75th percentiles. The mini hollow square within the box plot represents the mean, where the hollow circle represents the median of the data. Our one sample t-test revealed right parietal nerve activity in the presence of 1000 nM 2-methylquinoline treatment was not significantly different than control ($p=0.18$ $n=10$).